IEEE Access
Multidisciplinary | Rapid Review | Open Access Journal

Received April 24, 2019, accepted May 15, 2019, date of publication May 30, 2019, date of current version June 13, 2019.

Digital Object Identifier 10.1109/ACCESS.2019.2919981

Impulsive Gear Fault Diagnosis Using Adaptive Morlet Wavelet Filter Based on Alpha-Stable Distribution and Kurtogram

MANG GAO, GANG YU, AND TAO WANG

School of Mechanical Engineering and Automation, Harbin Institute of Technology at Shenzhen, Shenzhen 518055, China

Corresponding author: Gang Yu (gangyu@hit.edu.cn)

This work was supported by the Shenzhen Basic Research Project under Grant JCYJ20130329143834246.

ABSTRACT The vibration signals extracted from gearbox are usually masked in heavy background noise. Analyzing the feature components of these signals is challenging and crucial to incipient fault diagnosis. The Kurtogram has been verified as a very powerful and practical tool in the mechanical fault diagnosis due to its advantages in detecting and characterizing transients in signals. However, the accuracy of the kurtogram is limited because it is based on short-time Fourier transform (STFT) or FIR filter in extracting transient characteristics from a noisy signal. Therefore, it is necessary to develop a more accurate filter to overcome its shortcomings and further improve its fault detection accuracy. Wavelet transform has been widely applied in the past as a powerful tool to analyze the non-stationary signals, and an alpha-stable distribution model is often used to describe the statistical features of non-Gaussian signals. In this paper, a Morlet wavelet filter is optimized based on the kurtogram and the alpha parameter of the alpha-stable distribution model. Through the analysis of simulation signals at different fault degrees and operating conditions, it can be concluded that alpha-stable distribution has better performance than kurtosis in measuring the non-Gaussian characteristics of an impulsive gear fault signal. The results obtained from the simulation and practical experiments confirm the superiority of the proposed method for incipient gear fault diagnosis.

INDEX TERMS Incipient fault diagnosis, kurtogram, Morlet wavelet, adaptive filter, alpha-stable distribution.

I. INTRODUCTION

Fault diagnostics and prognostics of gearbox are technically important and economically beneficial to avoid malfunctions and failures of rotating machinery in various engineering applications. Many techniques have been proposed in literature, for instance, vibration, oil debris, acoustic emission methods and thermal-based indication analysis, etc., among which vibration analysis is the most widely used and reliable method for fault diagnosis [1], [2]. The vibration signals are normally collected by an accelerometer which is mounted on the gearbox end cover plate or bearing bracket. However, it is not easy to reveal the correct information from the acquired signals directly [3]. Because the fault characteristics are usually submerged by the background noise, therefore, the main objective to diagnose the gear fault is how to extract fault characteristic data or information from vibration signals effectively.

A series of techniques have been developed to investigate the vibration signal for fault diagnosis, such as empirical mode decomposition (EMD), matching pursuit and time-scale method [4]{Wang, 2010 #23} and FFT-based techniques. Wavelet analysis is one of the effective approaches, especially for non-stationary signal processing and fault diagnosis. Yan *et al.* [5] investigated the applications of the wavelet analysis to diagnose rotary machine faults, including various fault extractions such as de-noising, extraction of unnecessary signals, and signal decomposition capability enhancement. The Morlet wavelet is a signal enveloped by a Gaussian function in frequency domain, and it is a cosine signal that decays exponentially in both directions just like an impulse, which makes it similar to a mechanical fault impulse. Hence many researchers utilized it to extract fault features. An adaptive Morlet wavelet filter based on kurtosis maximization was proposed to detect periodic impulses

The associate editor coordinating the review of this manuscript and approving it for publication was Mark Kok Yew Ng.

automatically for recognition of gear tooth fatigue crack [6]. Liu *et al.* [7] proposed an adaptive spectral kurtosis filtering method to extract the transient signals primarily based on Morlet wavelet. Upon the foundations of Morlet wavelet, many enhanced and synthetical algorithms have also been developed [8], [9]. Fan *et al.* [10] proposed a sparse representation of transients in wavelet basis to extract fault features in gearbox, however the calculation speed of the proposed method is limited due to the larger interval range and the smaller step of the parameter subset. Interestingly, a new family of model-based impulsive wavelets is constructed according to the theory of underdamped vibration system [11]. As a kind of novel sparse representation method for rolling bearing fault diagnosis, it provides an alternative to extract fault features in rotary machines.

In vibration analysis, a number of methods based on statistical measures, such as entropy [12], have been developed on the basis of classic statistical signal processing theory. These methods are focused on acquiring information such as non-Gaussian property and time-dependent characteristics [13]. Dyer [14] pointed out that bearing signals with faults follow non-Gaussian probability distribution, which could not be described by existing parameter probability models. Traditionally local statistics—kurtosis was used to measure the non-Gaussian characteristics and the higher kurtosis value means the greater possibility of mechanical fault. Many diagnostic methods based on derivative kurtosis indices also emerged, such as spectral kurtosis (SK) and fast kurtogram. Antoni *et al.* [15], [16] and Antoni and Randall [17] conducted in-depth research on SK. They generalized it and extended the definition of ''kurtogram'' to a broader range of non-stationary signals. Because of the advantage of extracting transient components in noise signal, kurtogram has been proved to be a very powerful and practical tool in mechanical fault diagnosis, and many researchers have investigated related or enhanced approaches [18]–[21]. However, the accuracy of kurtogram is limited because it is based on short-time Fourier transform (STFT) or FIR filter in extracting transient characteristics from a noisy signal [7], [22].

In order to get over the shortcomings of kurtogram, more accurate filters should be developed. The newly proposed infogram by Antoni [23] intended to capture the signature of repetitive transients in both time and frequency domains, which extended the domain of applicability of the kurtogram significantly. Gu *et al.* [24] combined the infogram and a novel Pareto-based Bayesian approach to extract repetitive transients. Other improved indexes were also put forward, such as protrugram, which was first time proposed by Barszcz and JabŁoński [25] as an alternative to kurtogram. Qin *et al.* [26] proposed an improved kurtosis and iterative thresholding algorithm to detect the transient feature of faulty wind turbine planetary gearboxes. However, seldom could these indexes be used to extract the incipient fault features.

Yu et al. first proposed an approach using alpha-stable distribution to describe the impulse nature of bearing fault signals, and a new bearing fault detection method based on kurtogram and α parameter of alpha-stable model was put forward, which has better performance on detecting incipient bearing faults than that based on the traditional kurtogram [27].

In this paper an alpha-stable distribution model is proposed to describe the statistical features of gear fault signals. Different from the method proposed in Ref. [27], α parameter of alpha-stable model is chosen as a new criterion to optimize the suitable Morlet wavelet parameters to de-noise the fault signals, and thus performs better in incipient fault feature extraction. In order to reduce the time-consuming computation for searching the whole frequency scope, the fast kurtogram is applied for obtaining the initial center frequency range.

The primary contributions of this paper are summarized as follows:

- It is the first time to propose a new criterion based on alpha-stable distribution to optimize the adaptive Morlet wavelet filter parameters.
- The α parameter and other 3 parameters of alpha-stable distribution as well as the kurtosis are compared as criteria to represent the gear faults from 3 different aspects.
- Fast kurtogram is employed to determine the approximate fault frequency band to reduce the computation time for the first time.

This paper includes six sections. Introduction is given in Section 1. Section 2 introduces the basic philosophy of Morlet wavelet as well as alpha-stable distribution. To detect the gear fault signal, a simulation model of the transient signal is explained and the performance of the alpha-stable parameters and kurtosis under different working conditions is investigated. A new method based on kurtogram and the alpha-stable distribution parameter and adaptive Morlet wavelet is proposed. The verification of the performance of the proposed method by both simulation and experiments is presented in Section 3 and Section 4 respectively. The results are compared with Morlet wavelet filter based on the optimization of maximum kurtosis and fast kurtogram. It has been validated that the proposed approach is an effective method to detect the gear fault in initial stage. Section 5 presents a discussion about this research and further explain the reason why the proposed method is superior to current approaches. Finally, Section 6 gives brief conclusions.

II. THE PRINCIPLE OF PROPOSED METHOD

A. BASIC CONCEPT OF WAVELET TRANSFORM AND MORLET WAVELET

Wavelet transform is a mathematical technique which changes a time domain signal into a time-scale domain. Wavelet transform is determined by performing dilation and translation of mother wavelet $\psi(t)$.

$$\psi_{a,b}(t) = |s|^{-\frac{1}{2}} \psi\left(\frac{t-\tau}{s}\right) s, \quad \tau \in R; s \neq 0 \qquad (1)$$

where s, τ represent scale factor and time location, the $|s|^{-1/2}$ factor is applied for energy conservation. The scale parameter $s > 0$, and $\tau \in R$ could be continuous or discrete.

The wavelet transform of a finite energy signal $x(t)$ is actually the convolution of $x(t)$ and a conjugated wavelet:

$$W(s,\tau) = |s|^{-1/2} \int_{-\infty}^{\infty} x(t)\psi^*\left(\frac{t-\tau}{s}\right) dt \tag{2}$$

where $\psi^*(t)$ is the complex conjugation of $\psi(t)$.

When a fault exists in the rotary components such as a gear or bearing of a mechanical system, periodic impulses are generated. As a Morlet wavelet is similar to an impulse component in a fault signal, it is usually used to detect fault features [6]–[8]. A Morlet wavelet (only with real part, actually a Morlet wavelet is a complex exponential function) is defined as [7]:

$$\psi(t) = \exp\left(-\frac{f_b\,[2\pi f_c(t-\tau)]^2}{\sqrt{1-f_b^2}}\right)\cos\left[2\pi f_c(t-\tau)\right] \tag{3}$$

where, f_b means the damping ratio which is also known as decaying factor, f_c is the central frequency, and τ represents the time parameter. By dilating with f_c, f_b and moving with τ, a series of daughter wavelets can be attained.

The frequency domain is as follows:

$$\varphi(f) = \exp\left(-\frac{\sqrt{1-f_b^2}}{f_b\,(2\pi f_c)^2}\,(f-f_c)^2\right) \tag{4}$$

Actually, the Morlet wavelet in the frequency domain is a Gaussian window, the central frequency f_c in the Eq.(3) is the center coordinate of the Gaussian peak, and f_b represents the decaying trend of the Gaussian window which controls the shape of the frequency. The bigger the value of f_c is, the higher the central frequency will be. Meanwhile, the smaller the value of f_b, the steeper the curve [7].

B. THE ALPHA-STABLE DISTRIBUTION

In general, alpha-stable distribution explains a specific group of random signals, including a significant impulsive waveform as well as probability density. Since no closed-form probability distribution function (PDF) expression exists, the alpha-stable distribution can be expressed by its characteristic function as proposed in Refs. [27]–[29]:

$$\varphi(t) = \exp\left\{jAt - \gamma\,|t|^{\alpha}\,[1 + j\beta sign(t)\,\omega(t,\alpha)]\right\} \tag{5}$$

where

$$\omega(t,\alpha) = \begin{cases} \tan\dfrac{\alpha\pi}{2} & \alpha \neq 1 \\ \dfrac{2}{\pi}\log|t| & \alpha = 1 \end{cases}$$

$$sign(t) = \begin{cases} 1 & t > 0 \\ 0 & t = 0 \\ -1 & t < 0 \end{cases}$$

It can be seen that the stable characteristic function contains four parameters: α, β, γ and A. α is known as characteristic index ($0 < \alpha \leq 2$). A represents location parameter ($-\infty < A < \infty$), and it is the mean value of alpha-stable distribution when $1 < \alpha \leq 2$, and the median when $0 < \alpha < 1$. β is a symmetry parameter ($-1 \leq \beta \leq 1$). γ stands for a scale parameter ($\gamma > 0$), known as dispersion coefficient.

Since parameters α, β, γ and A determine the alpha-stable distribution, it is very essential to obtain their valid and accurate values. There are many numerical parameters estimate methods, such as the Quantile method, the maximum likelihood (ML) method, and the characteristic function (CF) method [30], [31]. The Ref. [32] has confirmed the idea that the stable distribution hypothesis for a signal is supported if three estimated results are close. In this paper, the Quantile method is selected to estimate alpha-stable parameter values. Please refer to Ref. [27] for more details about obtaining parameters of alpha-stable distribution.

C. SIMULATION OF GEAR FAULT SIGNALS

A simulation of a gear fault signal is given in this section for the following study. Actually, the impulsive gear fault is usually a transient. Hence, the fault signal $y(t)$ can be simulated by the linear overlap of a transient signal and a Gaussian noise [7].

$$y(t) = x(t) + A_n n(t) \tag{6}$$

And

$$x(t) = (1 + 0.6\cos[2\pi f_n(t-\tau_n)])\sum_{m=0}^{M} h(t-kT_0) \tag{7}$$

where $n(t)$ represents a Gaussian noise and the amplitude value is 0.36, $x(t)$ stands for the transient signal, $h(t)$ is an impact impulses function and k, T_0 are the number of transients and time period, respectively. To be specific, $h(t)$ can be expressed as:

$$h(t) = \begin{cases} A_m \exp\left(-\frac{\varsigma[2\pi f_0(t-\tau)]}{\sqrt{1-\varsigma^2}}\right)\cos[2\pi f_0(t-\tau_0)] (t \geq \tau_0 + kT_0) \\ 0(else) \end{cases} \tag{8}$$

where ς is a decaying factor and f_0 is the transient feature frequency. Sampling frequency and time are chosen as 2000 Hz and 1s separately.

According to the Eq. (7), the realistic simulation results can be obtained after setting reasonable parameters and all values of parameters are shown in Table 1.

The simulation signal according to the above equations and parameters is shown in Fig. 1:

D. VARIATIONS OF ALPHA-STABLE DISTRIBUTION PARAMETERS UNDER DIFFERENT GEAR FAULT CONDITIONS

When a fault exists, kurtosis is often used to describe the non-Gaussian vibration signals. In this section, alpha-stable

TABLE 1. The parameters applied in the simulation signal.

f_n (Hz)	f_0 (Hz)	ς	T_0 (s)	τ_0 (s)	τ_n (s)	A_m	A_n	k
0.85	200	0.05	0.2	0.1	0.1	0.8,0.7,1,0.7,0.9	0.36	0:4

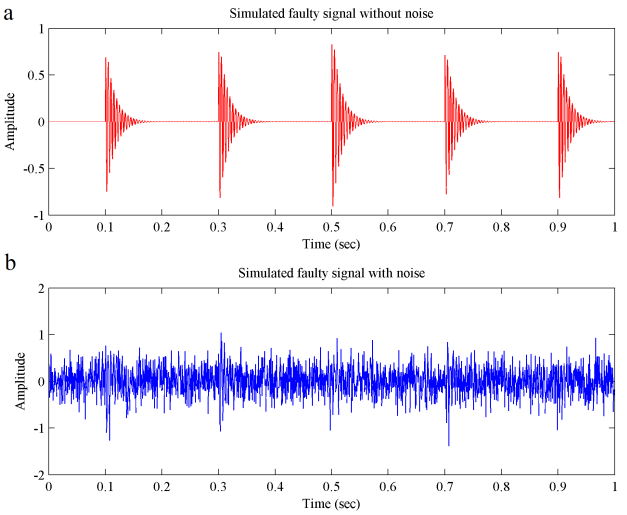

FIGURE 1. Gear fault simulation signal with and without noise. a) simulated fault signal without noise, b) simulated fault signal with noise.

distribution parameters are analyzed as a comparison to kurtosis under different gear fault conditions.

E. THE INFLUENCE OF FAULT DEGREE

The parameter A_m in impulse Eq. (8) represents the fault degree. In order to investigate the influences of fault degree on the parameters ($kurtosis, \alpha, \beta, \gamma, A$), A_m is set to increase from 0.1 to 6.35. Other parameters remain the same in Table 1. 1500 simulation signals are generated to represent the changes of fault degree [33]. Fig. 2 shows the changing results of alpha parameters and kurtosis values while the fault degree increases.

From Fig. 2, the following results can be drawn:

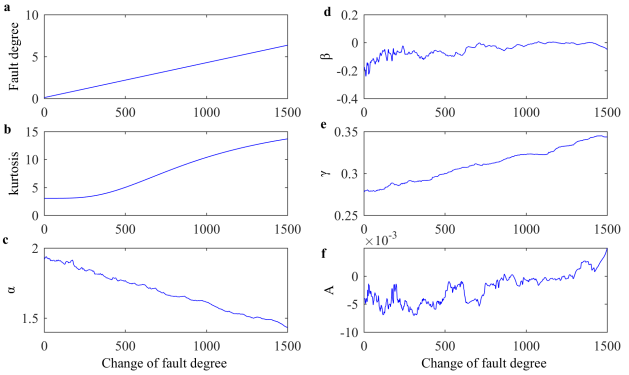

FIGURE 2. Changing results of alpha parameters and kurtosis along with the increase of fault degree. a) the change of fault degree of 1500 simulation signals, b) the change of kurtosis value along with the increase of fault degree, c) the change of α value along with the increase of fault degree, d) the change of β value along with the increase of fault degree, e) the change of γ value along with the increase of fault degree, f) the change of A value along with the increase of fault degree.

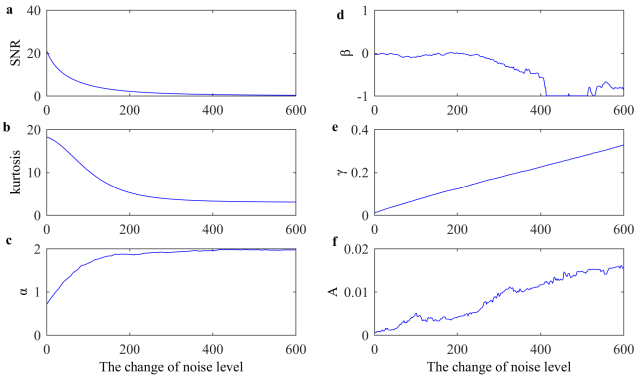

FIGURE 3. Changing results of alpha parameters and kurtosis with changing SNR. a) the value of SNR with the change of noise level, b) the change of kurtosis value along with the decrease of SNR, c) the change of α value along with the decrease of SNR, d) the change of β value along with the decrease of SNR, e) the change of γ value along with the decrease of SNR, f) the change of A value along with the decrease of SNR.

1) When gear fault degree changes, kurtosis and α can both represent the fault features of the gear signal. When fault degree increases, values of kurtosis increase, while α values decrease.
2) Before the 300th point, kurtosis values keep stable, while the values of α decrease monotonously, which indicates that in representing incipient fault, α is better than kurtosis.
3) The changes of the other three alpha-stable parameters can't describe the gear fault degree in well manner.

F. THE INFLUENCE OF THE SIGNAL TO NOISE RATIO

Signals acquired directly in the gearbox inevitably contain background noise. If the noise amplitude is high, the gear meshing signals are relatively weak and vice versa. In order to analyze the effect of noise upon the alpha-stable parameters, noise level is set to increase linearly. Similar to previous analysis, the parameter A_n in Eq. (6) is set as [0.01, 0.4]. 600 simulation signals with different SNR are generated. The results of the simulation are shown in Fig. 3.

Form Fig. 3, it has been observed that:

1) With the decreasing of SNR (noise increase), both kurtosis and α have a rapid change before point 200. When the noise becomes stronger, both of them tend to be stable.
2) The above change trend indicates that when the noise increases to some degree, both kurtosis and α become insensitive to noise.
3) The variation in β cannot describe the gear fault degree in a good way, A increases overall, but its values fluctuate at small scopes. γ goes smoothly.

G. THE INFLUENCE OF GEAR ROTATIONAL SPEED

The gear fault signal varies as the rotational speed of gearbox changes. In this simulation, the rotational speed increases linearly to determine the impact of speed on alpha-stable parameters and kurtosis. To be specific, 60 signals are generated under increasing speeds condition, the maximum value

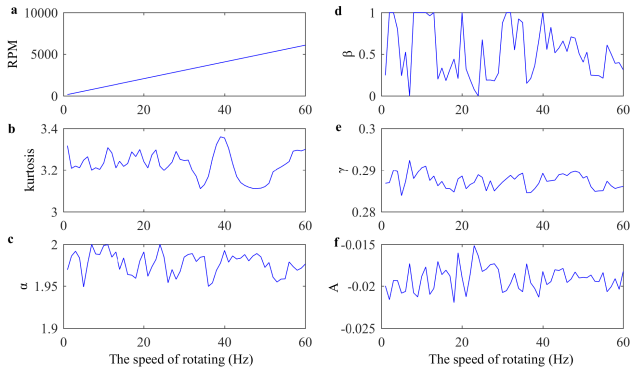

FIGURE 4. Changing results of alpha parameters and kurtosis with different rotational speeds. a) the change of rotational speed of 60 simulation signals, b) the change of kurtosis value along with the increase of rotational speed, c) the change of α value along with the increase of rotational speed, d) the change of β value along with the increase of rotational speed, e) the change of γ value along with the increase of rotational speed, f) the change of A value along with the increase of rotational speed.

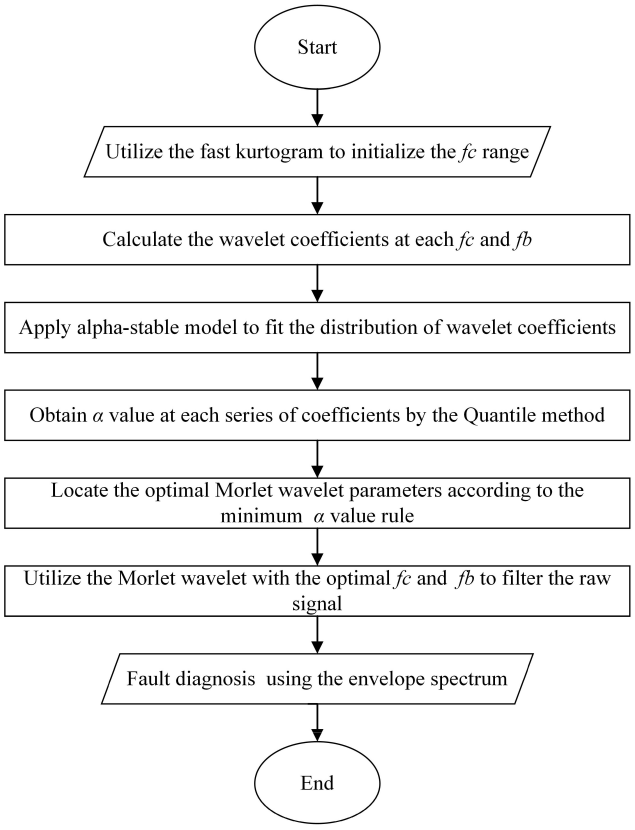

FIGURE 5. Flow chart of the proposed method.

of parameter $k+1$ in Eq. (7) represents the impulse number per second, therefore, the speed change can be achieved by tuning the value of k. k is set as [1, 100]. The results of the speed influence are shown in Fig. 4.

From Fig. 4, it is hard to tell their differences of these parameters. In order to compare their superiority, the variance of the corresponding alpha-stable parameters and kurtosis are obtained and shown in Table 2.

TABLE 2. Variances of alpha-stable parameters and kurtosis.

Parameter	Quantity Variance
α	1.7299×10^{-4}
β	0.1010
γ	3.3403×10^{-6}
A	2.0760×10^{-6}
Kurtosis	0.0041

From Table 2, two valid conclusions can be drawn as follows:

1) In comparison to kurtosis, the variance of α is far smaller. Hence as a criterion, α is less influenced by rotating speed.
2) As for the changes of the remaining three alpha-stable parameters, β has too large variances, while β perform very well comparing to the other parameters.

In conclusion, α and kurtosis can both represent fault degree, while in early stage, α outweighs kurtosis. β, γ, A do not show an obvious linear relationship with the fault degree, hence they can't be used as criteria to represent the gear fault, even though they are not sensitive to rotating speed. In SNR simulation experiment, α and kurtosis are almost the same. While in rotating speed factor, kurtosis is more easily affected by speed.

Therefore, the overall performance of α is superior to kurtosis.

H. THE PROPOSED ADAPTIVE MORLET WAVELET FILTER BASED ON THE ALPHA-STABLE DISTRIBUTION PARAMETER

Based on the analysis in the previous section, it is found that the α value is an excellent criterion to describe the valuable fault information of a Non-Gaussian signal. However, searching in the whole frequency domain requires time-consuming computation, hence fast kurtogram is employed to initialize the central frequency f_c range. In order to de-noise the original signal with the optimal Morlet wavelet based on kurtogram and the alpha-stable distribution parameter (minimum α value), the steps of finding optimal Morlet wavelet parameters and utilizing them to extract the fault features are summarized as follows:

1) Utilize the fast kurtogram to preprocess the raw signal and get the initial searching range of central frequency f_c;
2) Calculate the wavelet coefficients about the signal and daughter wavelet at each central frequency f_c and decaying factor f_b (f_c, f_b is from Eq.(3));
3) Apply alpha-stable model to fit the distribution of wavelet coefficients at each f_c and f_b. Using the Quantile method, α value is obtained at each series of coefficient;
4) According to the principle of minimum α value, locate the optimal Morlet wavelet parameters f_c and f_b that matches the frequency of signal transients feature best;

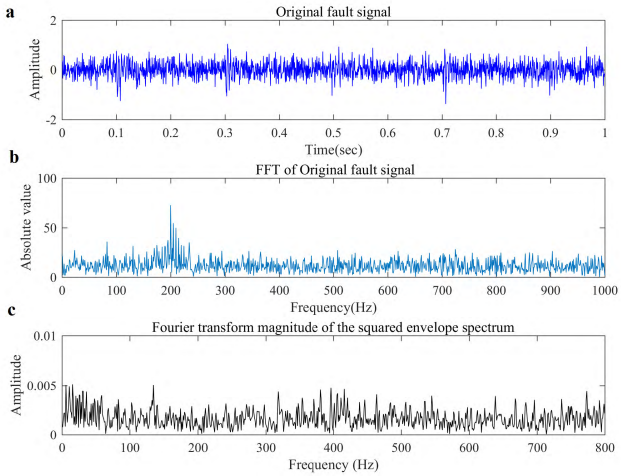

FIGURE 6. (a) Time waveform of the original simulation signal, (b) frequency spectrum of the original simulation signal, (c) squared envelope spectrum of the original simulation signal.

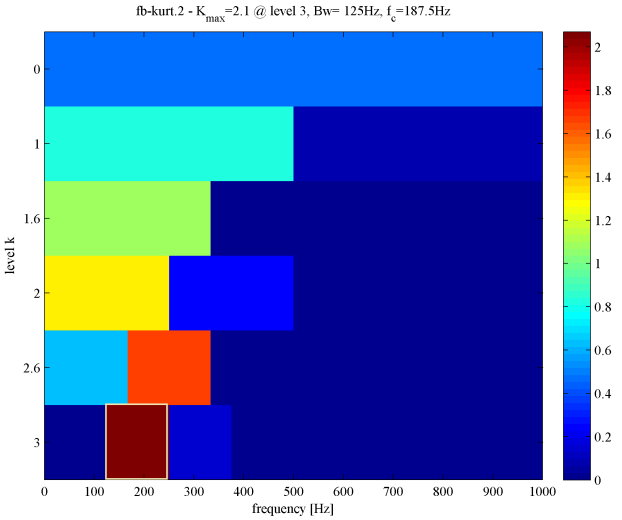

FIGURE 7. Fast kurtogram analysis of the simulated gear fault signal.

5) Utilize the Morlet wavelet with the optimal f_c and f_b to filter the raw signal;
6) Find the fault features using envelope spectrum.

The flow chart is shown in Fig. 5.

III. SIMULATION ANALYSIS

According to the gear fault simulation signal introduced in Section 2, the frequency spectrum and envelope spectrum of the simulation signal are given in Fig. 6. From these graphs, it is difficult to get any useful information of faults, so the proposed approach is utilized to address the fault signal with noise.

Firstly, the fast kurtogram is applied, the decomposition levels is set from 1 to 3 (the detailed procedure of kurtogram decomposition please refer to Ref. [16]), and the result is presented in Fig. 7.

From Fig. 7, it can be seen that the central frequency is 187.5 Hz, and the bandwidth is 125 Hz. Therefore, the

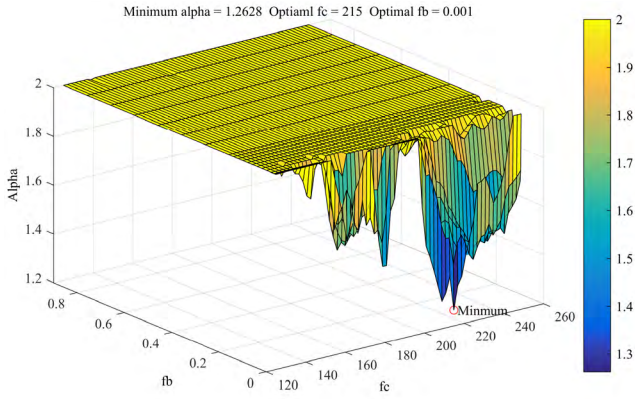

FIGURE 8. The optimal central frequency and decaying factor based on minimum α value criterion.

initial searching range of central frequency f_c is {125, 250}, the searching step length is set as 2. Since the selection of searching range and step length is highly related to the speed and accuracy of the method, therefore, a balance between efficiency and accuracy should be guaranteed [34]. The changing step of f_b is non-uniform, which aims to provide higher resolution at lower damping ratio values, and keep relatively high efficiency of the method. f_b aims at specifying meshing damping ratio, and according to Ref. [35], the damping ratio varies from 0.03 to 0.17. Hence, the range of f_b is chosen as {{0.001:0.002:0.01} {0.02:0.02:0.2} {0.3:0.1:0.9}} which have small steps in the low value range and large steps in the high value range. In the process of obtaining wavelet coefficient, the time shift is set as 200 steps. Then the minimum α value criterion is utilized to optimize f_c and f_b, and the result is shown in Fig. 8.

From Fig. 8, the optimal f_c and f_b are obtained, and the optimal Morlet wavelet is used to filter the raw signal to get the envelope of the filtered signal. The results are illustrated in Fig. 9. The squared envelope spectrum of the processed signal is also given, which is shown in Fig. 10.

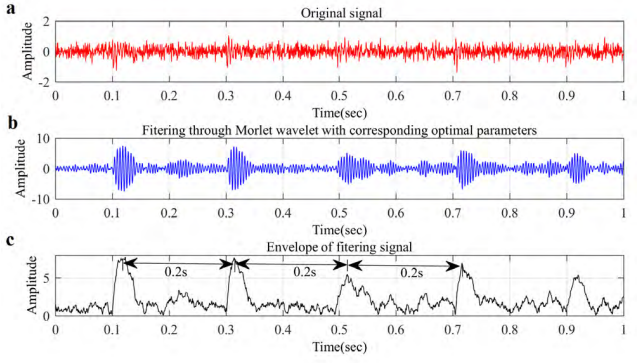

FIGURE 9. Simulation fault signal processed by proposed method: (a) original signal, (b) signal after filtering by Morlet wavelet, (c) the envelope of the processed signal.

From Fig. 9, it is obvious that the periodical impulse components are clearly identified. The fault characteristic frequency fr and its frequency multiplication as shown

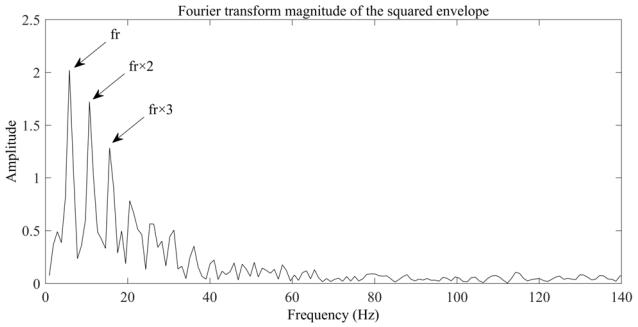

FIGURE 10. The squared envelope spectrum of the processed signal based on the proposed method.

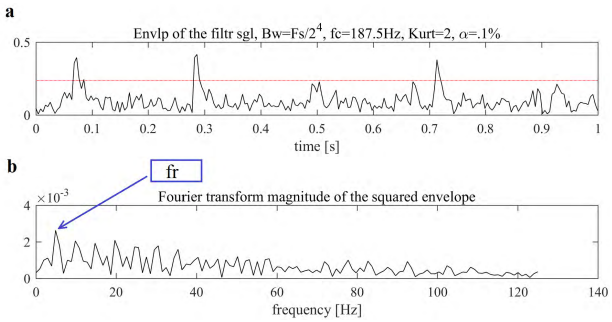

FIGURE 11. Simulation fault signal processed by fast kurtogram: (a) envelope of the processed signal, (b) envelope spectrum of the processed signal.

in Fig. 10 also indicate that the fault exists in the simulation signal. In order to make a comparison between the proposed method and fast kurtogram, the envelope and the envelope spectrum are also obtained by fast kurtogram, the result is shown in Fig. 11.

From Fig. 11(b), the fault characteristic frequency in the squared envelope spectrum is less obvious comparing with the proposed method. The amplitudes of the fault characteristic frequency shown in Fig. 10 are also larger than those in Fig. 11(b). Comparing results represented in Fig. 9(c) with Fig. 11(a), the impulse amplitudes in Fig. 9(c) are more obvious than those in Fig. 11(a). It is apparent that the proposed method is more effective than fast kurtogram in finding impulsive components of simulation signals. Comparative analysis with the adaptive Morlet wavelet filter based on the maximum kurtosis method proposed by Ref. [6] is also performed, the corresponding results are shown in Fig. 12 and Fig. 13.

From the results represented in Fig. 9(c) and Fig. 13(c), it is obvious that the proposed method also performs better than that based on the maximum kurtosis criterion under the same condition.

In order to further compare the two methods, the squared envelope spectrum of the processed signal based on kurtosis maximum criterion is also obtained, which is shown in Fig. 14.

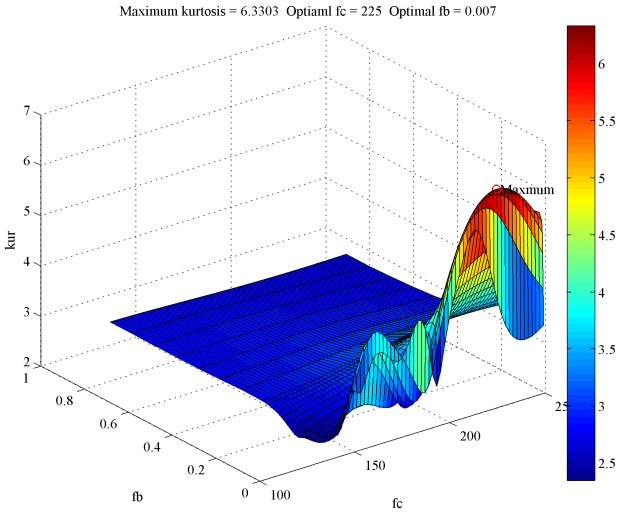

FIGURE 12. The optimal central frequency and decaying factor based on maximum kurtosis criterion.

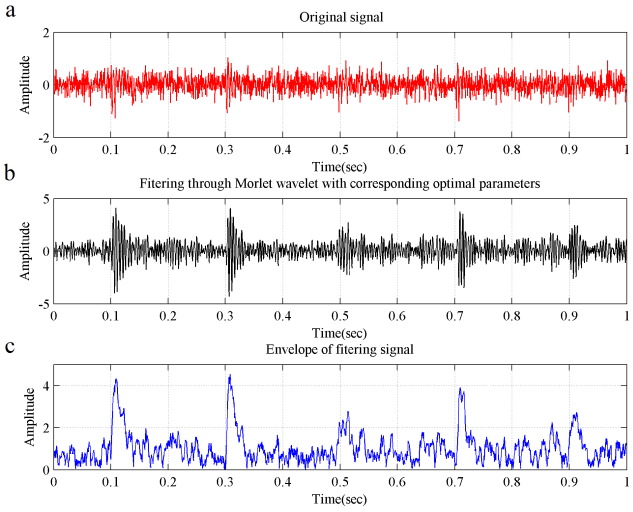

FIGURE 13. Simulation fault signal processed by kurtosis maximum criterion: (a) original signal, (b) signal after filtering by Morlet wavelet, (c) the envelope of the processed signal.

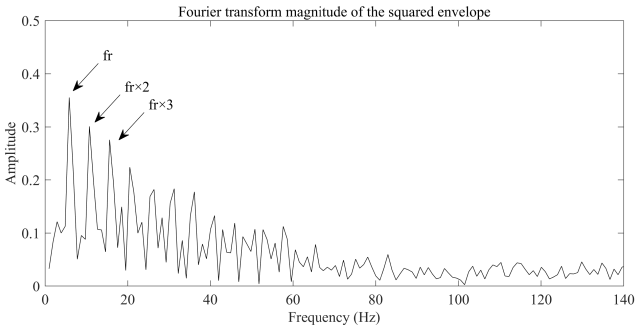

FIGURE 14. The squared envelope spectrum of the processed signal based on the maximum kurtosis criterion.

From Fig. 10 and Fig. 14, the fault characteristic frequency shown in Fig. 14 is the same as it is shown in Fig. 10. The amplitudes of the fault characteristic frequency shown in Fig. 10 are larger than those in Fig. 14. Thus the overall

TABLE 3. Time consumption of finding optimal parameters using the proposed method and kurtosis maximum criterion in different central frequency searching ranges.

Central Frequency Searching Range	Proposed Method(s)	Kurtosis Maximum Criterion(s)
{ 125:2:250 }	53.258	17.506
{ 100:2:500 }	121.315	64.021

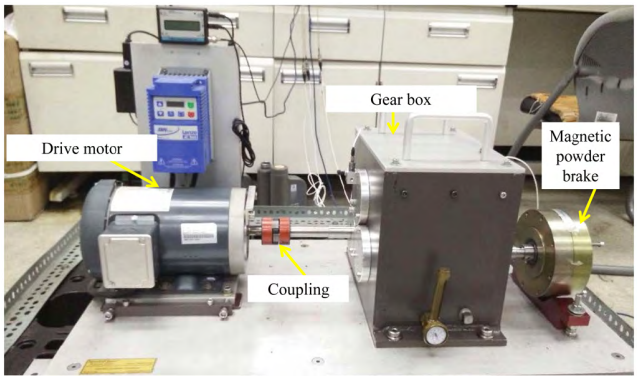

FIGURE 15. The test rig (GDS).

performance of the proposed method in envelope spectrum aspect is better than the kurtosis maximum criterion method to some degree.

The time consumption of finding optimal f_c and f_b about different methods in different searching ranges is also compared. {125:2:250} stands for the condition of employing the fast kurtogram to initialize the central frequency range, and {100:2:500} represents the condition without the fast kurtogram. The results are presented in Table 3.

From Table 3, it can be found that the time consumption of the proposed method is larger than that based on kurtosis maximum criterion at the same searching range. With the application of fast kurtogram to initialize the searching range of central frequency, the computation time decreases significantly by both the proposed method and the kurtosis maximum criterion method. Therefore, employing the fast kurtogram is efficient and necessary.

IV. EXPERIMENTAL VERIFICATION

A. CASE STUDY 1

The test gearbox (Gearbox Dynamics Simulator (GDS) from Spectra Quest Company as shown in Fig. 15) has three parallel shafts which can achieve two-stage gear transmission. A gear with half of a tooth removed is used as a simulation of tooth broken fault for this experiment. The fault gear is set at the intermediate shaft. The inner structure of the gearbox and gear fault are presented in Fig. 16.

The electric motor supplies power of 2.2 kw. The rotational speed of the input shaft is 1800 rpm, and the rotational frequency of the input shaft is 29.3 Hz. The number of teeth of faulted gear is 36, and meshing frequency of faulted gear is 305.9 Hz. And the periodical transient frequency of faulted

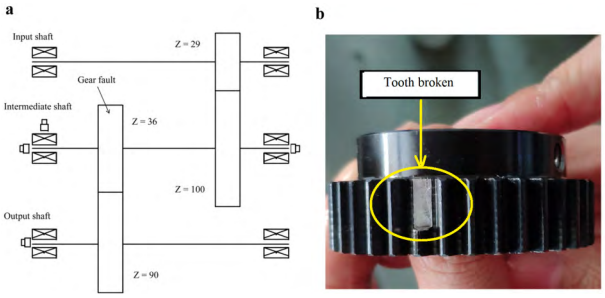

FIGURE 16. (a) The inner structure of the gearbox, (b) gear tooth broken fault.

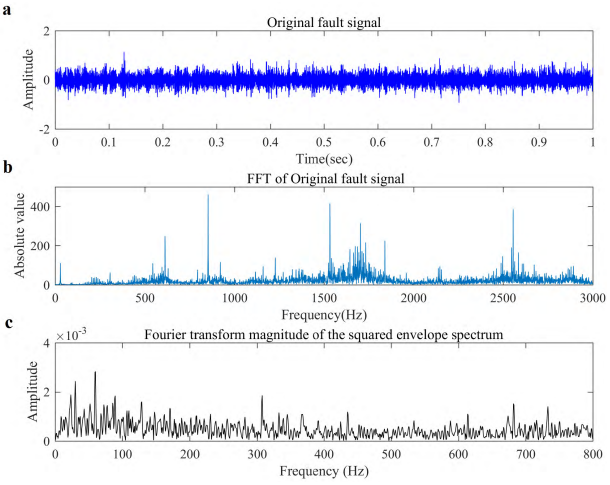

FIGURE 17. (a) Time waveform of the tooth broken fault signal, (b) frequency spectrum of the tooth broken fault signal, (c) squared envelope spectrum of the tooth broken fault signal.

gear is 8.5 Hz (0.117s). The gear fault vibration signal is collected at the sampling frequency of 12000Hz.

The time waveform of the original gear fault vibration signal, its corresponding frequency spectrum and its squared envelope spectrum are shown in Fig. 17.

From Fig. 17(b), (c), it is hard to find fault frequency. Thus, the conventional time frequency analysis can not detect the fault components. Other methods should be taken into consideration.

According to the procedure introduced earlier, the fast kurtogram is applied to find the initial range of f_c, with the decomposition levels setting from 1 to 6, the result is presented in Fig. 18.

From Fig. 18, it can be obtained that the initial central frequency f_c range is {350, 500}, the searching step is set as 2. In order to increase the searching efficiency as illustrated before, the range of f_b is selected as {{0.001:0.002:0.01} {0.02:0.02:0.2} {0.3:0.1:0.9}}, then the minimum α value criterion is applied to optimize f_c and f_b, the result is shown in Fig. 19:

From Fig. 19, the optimal f_c and f_b is obtained and then the optimal Morlet wavelet is used to filter the raw signal,

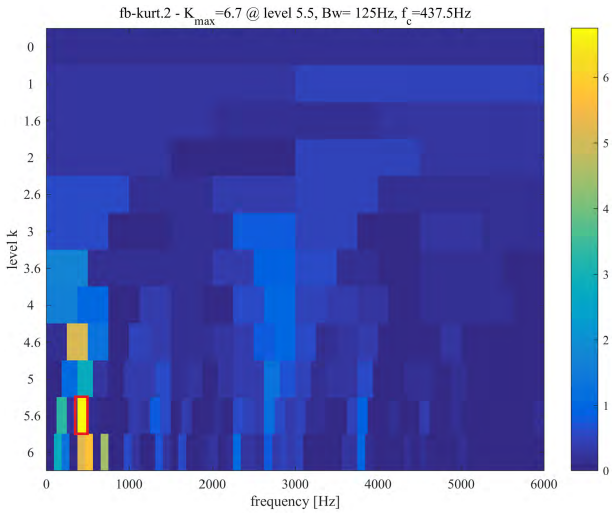

FIGURE 18. Fast kurtogram analysis of the tooth broken fault signal.

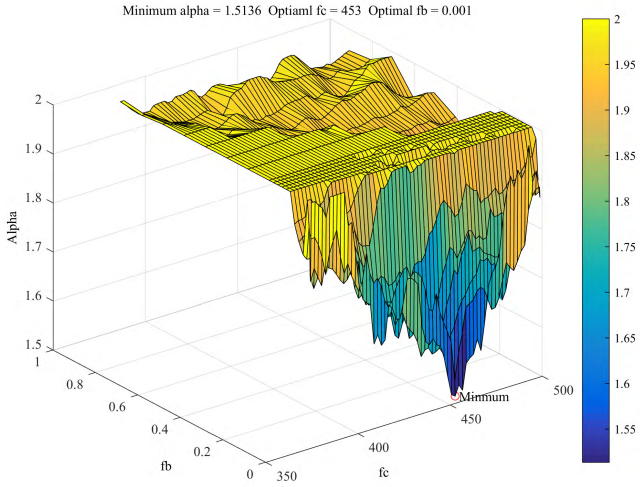

FIGURE 19. The optimal central frequency and decaying factor based on minimum α value criterion.

the envelope of the signal after filtering is obtained, the result is shown in Fig. 20:

From Fig. 20, it can be found that the periodical impulse components are clearly detected. The impulse period is equal to 0.117s, representing that the gear fault transients masked in noise are identified.

The squared envelope spectrum of the processed signal based on the proposed method can also be obtained as shown in Fig. 21, and it can be found that the fault characteristic frequency is clearly identified.

Then the comparison between the proposed method and fast kurtogram is conducted. The envelope spectrum is obtained by fast kurtogram as shown in Fig. 22.

Comparing the result presented in Fig. 22(a) with that in Fig. 20(c), it is easier for the proposed method to find out the periodical fault impulse components than fast kurtogram.

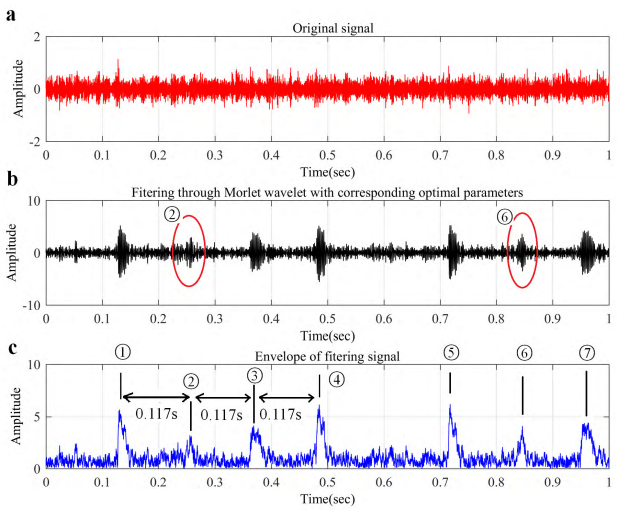

FIGURE 20. Tooth broken fault signal processed by proposed method: (a) original signal, (b) signal after filtering by Morlet wavelet, (c) the envelope of the processed signal.

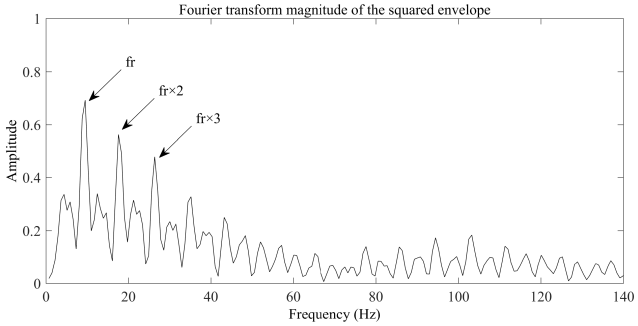

FIGURE 21. The squared envelope spectrum of the processed signal based on the proposed method.

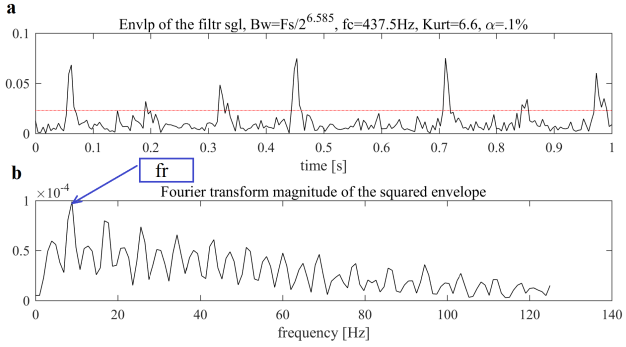

FIGURE 22. Tooth broken fault signal processed by fast kurtogram: (a) envelope of the processed signal, (b) envelope spectrum of the processed signal.

In Fig. 22(b), the fault characteristic frequency is less obvious than that with the proposed method.

Similarly, the results based on the adaptive Morlet wavelet filter proposed by Ref. [6] are also obtained as shown in Fig. 23 and Fig. 24. The squared envelope spectrum of the

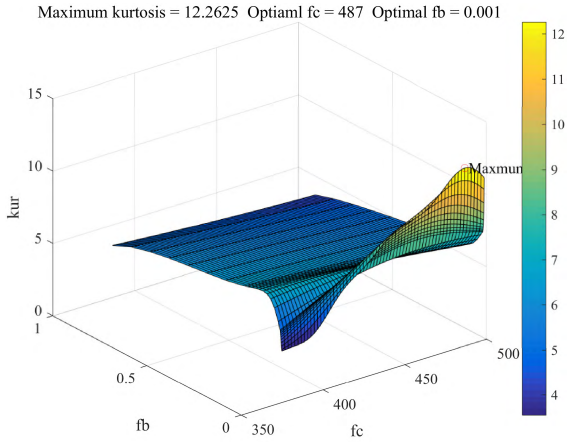

FIGURE 23. Obtain the optimal central frequency and decaying factor based on maximum kurtosis criterion.

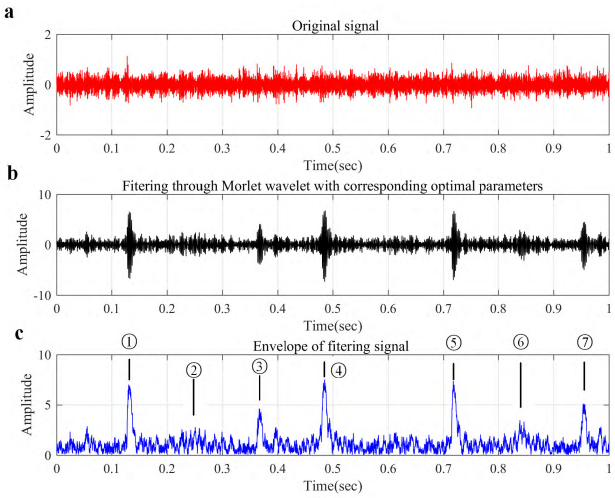

FIGURE 24. Tooth broken fault signal processed by kurtosis maximum criterion: (a) original signal, (b) signal after filtering by Morlet wavelet, (c) the envelope of the processed signal.

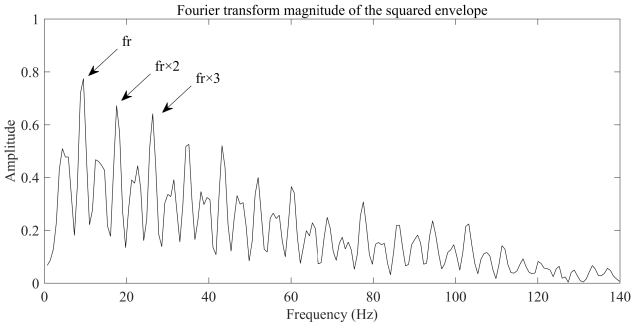

FIGURE 25. The squared envelope spectrum of the processed signal based on the maximum kurtosis criterion.

processed signal based on the kurtosis maximum method is also given, and it is presented in Fig. 25.

Comparing the results shown in Fig. 24(c) with that in Fig. 20(c), the second impulse in Fig. 24(c) is far less

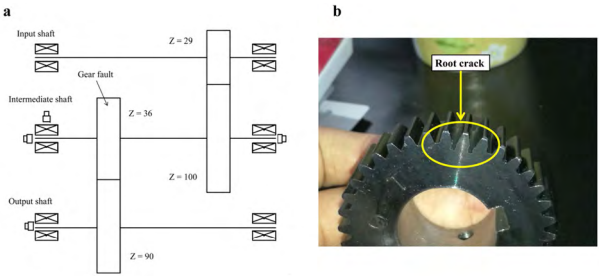

FIGURE 26. (a) The inner structure of the gearbox, (b) root crack broken fault.

obvious than that in Fig. 20(c), and it is almost masked in noise and hard to discern while the second impulse in Fig. 20(b) can be identified more clearly. Besides, the impulse which is marked with 6 in Fig. 24(c) is also hard to recognize. While in Fig. 20(c), the 6th impulse is quite clear and easy to identify. Therefore, the proposed method performs better than that based on the maximum kurtosis criterion under the same condition, especially in detecting incipient fault.

Comparing the squared envelope spectrum shown in Fig. 25 with Fig. 21, it can be found that the fault characteristic frequency in Fig. 21 is more obvious in respect to the frequency components of interference.

B. CASE STUDY 2

In order to further investigate the efficiency of the proposed method, another incipient fault is employed to validate the algorithm. In this case, the test rig is still the same as it is shown in the case study 1, however, the fault type is changed. The gear fault is root crack this time. A crack of 1 mm depth at the root of the intermediate shaft gear is used as a simulation of root crack fault for this experiment. The inner structure of the gearbox and gear fault are presented in Fig. 26. The rotational speed of the input shaft is 2400 rpm, and the rotational frequency of the faulted gear is 40 Hz. The number of teeth of faulted gear is 36, and meshing frequency of faulted gear is 417.6 Hz. And the periodical transient frequency of faulted gear is 11.5 Hz (0.087s). The gear fault vibration signal is collected at sampling frequency of 5120Hz.

The time waveform of the original gear fault vibration signal and its corresponding frequency spectrum are shown in Fig. 27.

According to the procedure introduced earlier, the fast kurtogram is applied to find the initial range of f_c, with the decomposition levels setting from 1 to 5, the result is presented in Fig. 28.

From Fig. 28, it can be found that the initial central frequency f_c range is $\{320, 480\}$, the searching step is also set as 2. In order to increase the searching efficiency as illustrated before, the range of f_b is selected as the same in case study 1, then the minimum α value criterion is utilized to optimize f_c and f_b, the result is shown in Fig. 29:

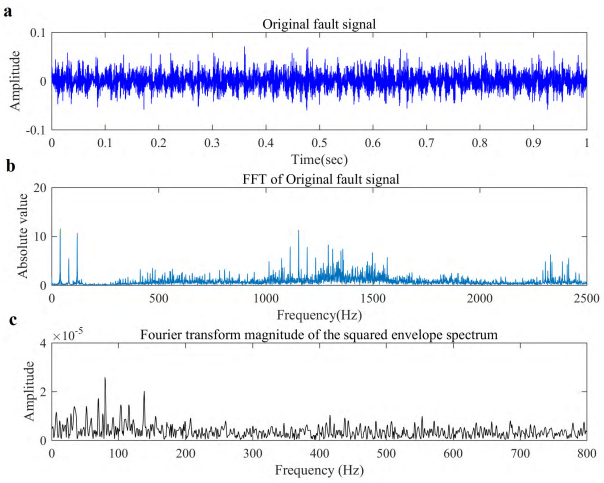

FIGURE 27. (a) Time waveform of the root crack fault signal, (b) frequency spectrum of the root crack fault signal, (c) squared envelope spectrum of the root crack fault signal.

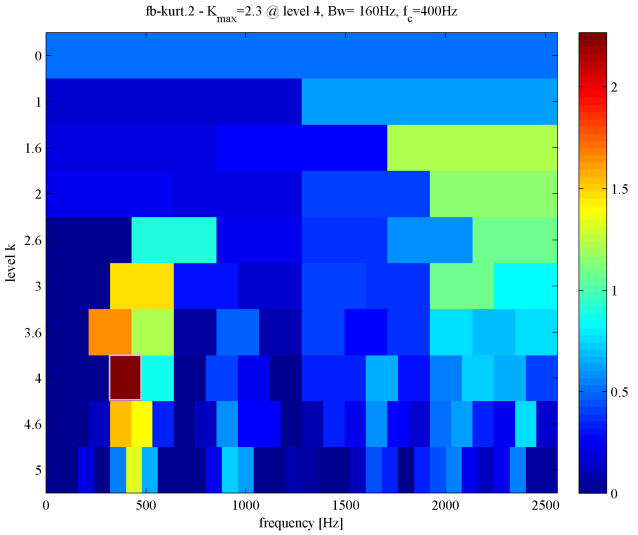

FIGURE 28. Fast kurtogram analysis of the root crack fault signal.

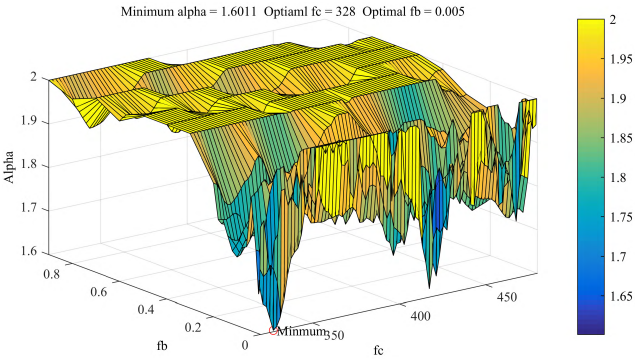

FIGURE 29. The optimal central frequency and decaying factor based on minimum α value criterion.

From Fig. 29, the optimal f_c and f_b are obtained and then the optimal Morlet wavelet is applied to filter the raw signal, the envelope of the signal after filtering is obtained, the result is shown in Fig. 30:

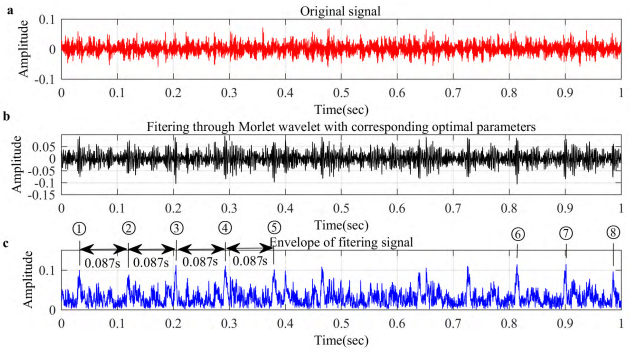

FIGURE 30. Root crack fault signal processed by proposed method: (a) original signal, (b) signal after filtering by Morlet wavelet, (c) the envelope of the processed signal.

From Fig. 30, it can be found that the periodical impulse components are clearly detected. The impulse period is equal to 0.087s, indicating that the gear fault transients submerged in noise are identified.

The squared envelope spectrum of the processed signal based on the proposed method can also be obtained as shown in Fig. 31, and it can be found that the fault characteristic frequency is clearly discerned. Therefore, the proposed method can be used to identify incipient gear fault through the squared envelope spectrum.

Then the comparison between the proposed method and fast kurtogram is conducted. The envelope and envelope spectrum obtained by fast kurtogram are shown in Fig. 32.

Comparing the result presented in Fig. 32(a) with Fig. 30(c), it is apparent that it is easier to find out the periodical fault impulse components with the proposed method than with fast kurtogram. Although the fast kutogram method could also detect the fault frequency in the squared envelope spectrum, the amplitude is far smaller than that as shown in Fig. 31.

Similarly, the results based on the kurtosis maximum criterion method are also obtained as shown in Fig. 33 and Fig. 34. The squared envelope spectrum of the processed signal based on the kurtosis maximum method can also be obtained, and it is presented in Fig. 35.

Comparing the results shown in Fig. 34(c) with Fig. 30(c), the second impulse in Fig. 34(c) is far less obvious than that in Fig. 17(c). The last impulse marked with 8 in Fig. 34(c) is also hard to recognize. While in Fig. 30(c), the last 3 impulses are quite clear and easy to identify. Therefore, the proposed method is better than that based on the maximum kurtosis criterion under the same condition. From the fault characteristic frequency in Fig. 35, it can be found that the characteristic frequency looks almost the same as it is presented in Fig. 31.

In order to further evaluate the performance quantitatively, characteristic power ratio (CPR) [36] is employed as:

$$CPR = {p_f}/{p_r} \tag{9}$$

where p_f is the fault frequency power, and p_r represents the residual power. The higher values of the CPRs indicate the

TABLE 4. The CPRs of the squared envelope spectra by different methods.

	Proposed Method	Maximum Kurtosis Criterion
Simulation case	0.5269	0.2228
Case 1	0.3122	0.2351
Case 2	0.2633	0.2507

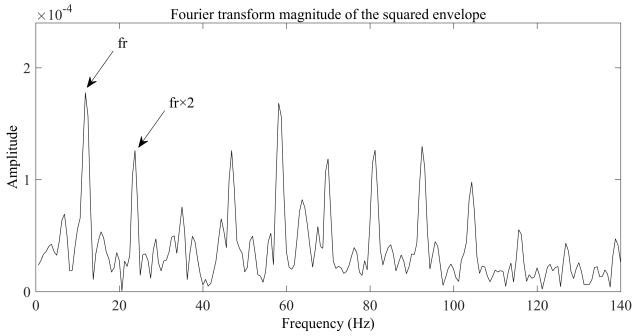

FIGURE 31. The squared envelope spectrum of the processed signal based on the proposed method.

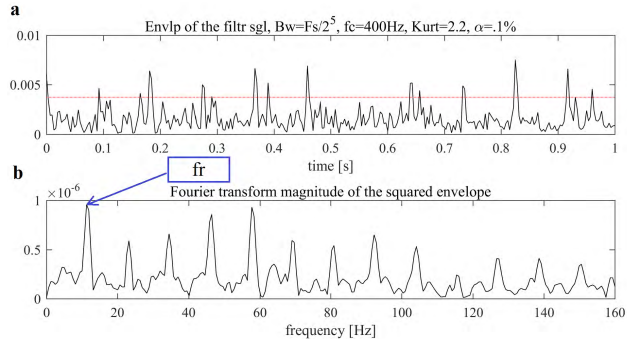

FIGURE 32. Root crack fault signal processed by fast kurtogram: (a) envelope of the processed signal, (b) envelope spectrum of the processed signal.

more obvious fault characteristic frequency. In other words, the performance is better.

By using Eq. (9), the CPRs of different methods are calculated and listed in Table. 4.

It can be seen that all CPRs of proposed method listed in Table. 4 are larger as compared to the corresponding CPRs of the maximum kurtosis criterion method, which indicates that the extracted fault features by proposed method is more obvious, and the proposed method is more effective for fault feature extraction.

V. DISCUSSION

Traditional methods, such as the fast kurtogram (based on short-time Fourier transform (STFT) or FIR filter) and adaptive Morlet wavelet filter based on maximum kurtosis criterion, are essentially a class of methods relying on the maximization of kurtosis for detecting the fault transients [6], [13]. Through the comparative analysis of kurtosis

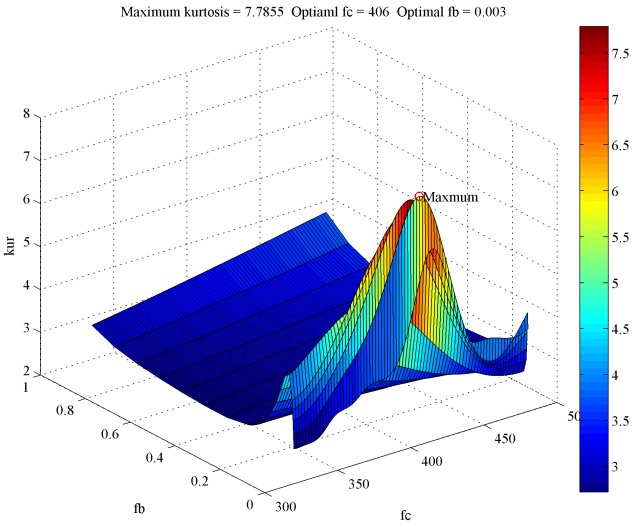

FIGURE 33. Obtain the optimal central frequency and decaying factor based on maximum kurtosis criterion.

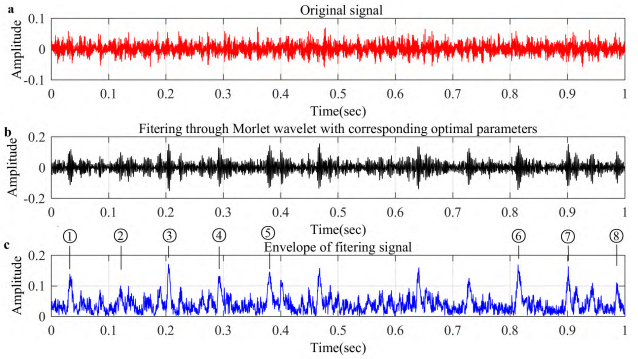

FIGURE 34. Root crack fault signal processed by maximum kurtosis criterion: (a) original signal, (b) signal after filtering by Morlet wavelet, (c) the envelope of the processed signal.

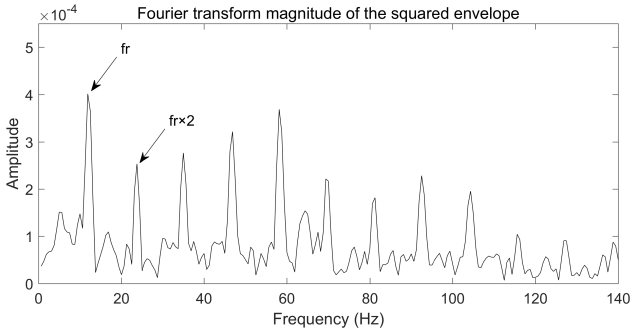

FIGURE 35. The squared envelope spectrum of the processed signal based on the maximum kurtosis criterion.

and α, it can be found that α is a more efficient and reliable parameter to describe incipient gear fault characteristics. Therefore, the proposed method is expected to perform better than traditional approaches.

However, the method solely relying on α to optimize the parameters of Morlet wavelet filter still has its drawbacks, because it requires time-consuming computation for search-

ing the whole frequency domain. Due to the application of tree structures, the frequency resolution of the fast kurtogram is limited, but it is very efficient to optimize the frequency band. Therefore, the fast kurtogram is employed to determine the approximate fault frequency, which can be used as the initial f_c range for further optimization of Morlet wavelet filter parameters based on the minimization of α.

VI. CONCLUSION

The paper presents a new fault diagnosis method based on adaptive Morlet wavelet with fast kurtogram and alpha-stable distribution to optimize its parameters. The alpha-stable parameter α value, as a criterion to describe the impulse nature of random signals, outweighs the traditional kurtosis. Fast kurtogram is employed to determine the approximate fault frequency band to reduce the computation time, and the minimization of α is utilized for further optimizing the parameters of Morlet wavelet filter. The performance of the proposed method in incipient gear fault diagnosis is verified both by simulation and experimental studies, which achieves more accurate and effective results than traditional methods. Future research will focus on investigating the potentials of utilizing alpha-stable distribution properties to enhance the diagnostic capabilities.

REFERENCES

[1] Y. Lei, J. Lin, M. J. Zuo, and Z. He, "Condition monitoring and fault diagnosis of planetary gearboxes: A review," *Measurement*, vol. 48, pp. 292–305, Feb. 2014.

[2] H. D. M. de Azevedo, A. M. Araújo, and N. Bouchonneau, "A review of wind turbine bearing condition monitoring: State of the art and challenges," *Renew. Sustain. Energy Rev.*, vol. 56, pp. 368–379, Apr. 2016.

[3] I. S. Bozchalooi and M. Liang, "A joint resonance frequency estimation and in-band noise reduction method for enhancing the detectability of bearing fault signals," *Mech. Syst. Signal Process.*, vol. 22, no. 4, pp. 915–933, May 2008.

[4] S. Wang, Z. K. Zhu, Y. He, and W. Huang, "Adaptive parameter identification based on morlet wavelet and application in gearbox fault feature detection," *EURASIP J. Adv. Signal Process.*, vol. 2010, no. 1, p. 101, 2010.

[5] R. Yan, R. X. Gao, and X. Chen, "Wavelets for fault diagnosis of rotary machines: A review with applications," *Signal Process.*, vol. 96, pp. 1–15, Mar. 2014.

[6] J. Lin and M. J. Zuo, "Gearbox fault diagnosis using adaptive wavelet filter," *Mech. Syst. Signal Process.*, vol. 17, no. 6, pp. 1259–1269, 2003.

[7] H. Liu, W. Huang, S. Wang, and Z. Zhu, "Adaptive spectral kurtosis filtering based on Morlet wavelet and its application for signal transients detection," *Signal Process.*, vol. 96, pp. 118–124, Mar. 2014.

[8] Y. Jiang, B. Tang, Y. Qin, and W. Liu, "Feature extraction method of wind turbine based on adaptive Morlet wavelet and SVD," *Renew. Energy*, vol. 36, no. 8, pp. 2146–2153, Aug. 2011.

[9] N. G. Nikolaou and I. A. Antoniadis, "Demodulation of vibration signals generated by defects in rolling element bearings using complex shifted Morlet wavelets," *Mech. Syst. Signal Process.*, vol. 16, no. 4, pp. 677–694, 2002.

[10] W. Fan, G. Cai, Z. K. Zhu, C. Shen, W. Huang, and L. Shang, "Sparse representation of transients in wavelet basis and its application in gearbox fault feature extraction," *Mech. Syst. Signal Process.*, vols. 56–57, pp. 230–245, May 2015.

[11] Y. Qin, "A new family of model-based impulsive wavelets and their sparse representation for rolling bearing fault diagnosis," *IEEE Trans. Ind. Electron.*, vol. 65, no. 3, pp. 2716–2726, Mar. 2018.

[12] Y. Li, X. Wang, Z. Liu, X. Liang, and S. Si, "The entropy algorithm and its variants in the fault diagnosis of rotating machinery: A review," *IEEE Access*, vol. 6, pp. 66723–66741, 2018.

[13] R. B. W. Heng and M. J. M. Nor, "Statistical analysis of sound and vibration signals for monitoring rolling element bearing condition," (in English), *Appl. Acoust.*, vol. 53, nos. 1–3, pp. 211–226, Jan./Mar. 1998.

[14] D. Dyer and R. M. Stewart, "Detection of rolling element bearing damage by statistical vibration analysis," (in English), *J. Mech. Eng.*, vol. 100, no. 2, pp. 229–235, 1978.

[15] J. Antoni, "The spectral kurtosis: A useful tool for characterising non-stationary signals," *Mech. Syst. Signal Process.*, vol. 20, no. 2, pp. 282–307, Feb. 2006.

[16] J. Antoni, "Fast computation of the kurtogram for the detection of transient faults," *Mech. Syst. Signal Process.*, vol. 21, no. 1, pp. 108–124, 2007.

[17] J. Antoni and R. Randall, "The spectral kurtosis: Application to the vibratory surveillance and diagnostics of rotating machines," *Mech. Syst. Signal Process.*, vol. 20, no. 2, pp. 308–331, 2006.

[18] D. Wang, P. W. Tse, and K. L. Tsui, "An enhanced Kurtogram method for fault diagnosis of rolling element bearings," *Mech. Syst. Signal Process.*, vol. 35, nos. 1–2, pp. 176–199, Feb. 2013.

[19] H. Wang, J. Chen, and G. Dong, "Fault diagnosis of rolling bearing's early weak fault based on minimum entropy de-convolution and fast Kurtogram algorithm," (in English), *Proc. Inst. Mech. Eng., C, J. Mech. Eng. Sci.*, vol. 229, no. 16, pp. 2890–2907, Nov. 2015.

[20] L. Wang, Z. Liu, Q. Miao, and X. Zhang, "Time-frequency analysis based on ensemble local mean decomposition and fast kurtogram for rotating machinery fault diagnosis," *Mech. Syst. Signal Process.*, vol. 103, pp. 60–75, Mar. 2018.

[21] X. Zhang, J. Kang, J. Zhao, J. Zhao, and H. Teng, "Rolling element bearings fault diagnosis based on correlated kurtosis kurtogram," (in English), *J. Vibroeng.*, vol. 17, no. 6, pp. 3023–3034, Sep. 2015.

[22] Y. Lei, J. Lin, Z. He, and Y. Zi, "Application of an improved kurtogram method for fault diagnosis of rolling element bearings," *Mech. Syst. Signal Process.*, vol. 25, no. 5, pp. 1738–1749, Jul. 2011.

[23] J. Antoni, "The infogram: Entropic evidence of the signature of repetitive transients," *Mech. Syst. Signal Process.*, vol. 74, pp. 73–94, Jun. 2016.

[24] X. Gu, S. Yang, Y. Liu, and R. Hao, "A novel Pareto-based Bayesian approach on extension of the infogram for extracting repetitive transients," *Mech. Syst. Signal Process.*, vol. 106, pp. 119–139, Jun. 2018.

[25] T. Barszcz and A. JabŁoński, "A novel method for the optimal band selection for vibration signal demodulation and comparison with the kurtogram," *Mech. Syst. Signal Process.*, vol. 25, no. 1, pp. 431–451, 2011.

[26] Y. Qin, J. Zou, and F. Cao, "Adaptively detecting the transient feature of faulty wind turbine planetary gearboxes by the improved kurtosis and iterative thresholding algorithm," *IEEE Access*, vol. 6, pp. 14602–14612, 2018.

[27] G. Yu, C. Li, and J. Zhang, "A new statistical modeling and detection method for rolling element bearing faults based on alpha–stable distribution," *Mech. Syst. Signal Process.*, vol. 41, nos. 1–2, pp. 155–175, 2013.

[28] M. Shao and C. L. Nikias, "Signal processing with fractional lower order moments: Stable processes and their applications," (in English), *Proc. IEEE*, vol. 81, no. 7, pp. 986–1010, Jul. 1993.

[29] E. F. Fama and R. Roll, "Parameter estimates for symmetric stable distributions," (in English), *J. Amer. Stat. Assoc.*, vol. 66, no. 334, pp. 331–338, 1971.

[30] I. A. Koutrouvelis, "Regression-type estimation of the parameters of stable laws," *J. Amer. Statist. Assoc.*, vol. 75, no. 372, pp. 918–928, 1980.

[31] J. H. McCulloch, "Simple consistent estimators of stable distribution parameters," *Commun. Statist. Simul.*, vol. 15, no. 4, pp. 1109–1136, 1986.

[32] J. P. Nolan, "Fitting data and assessing goodness-of-fit with stable distributions," Eng. Statist., Appl. Heavy Tailed Distrib. Econ., Washington, DC, USA, Tech. Rep., 1999.

[33] G. Yu and N. Shi, "Gear fault signal modeling and detection based on alpha stable distribution," in *Proc. Int. Symp. Instrum. Meas., Sensor Netw. Autom. (IMSNA)*, vol. 2, Aug. 2012, pp. 471–474.

[34] C. Shen, F. Liu, D. Wang, A. Zhang, F. Kong, and P. W. Tse, "A Doppler transient model based on the laplace wavelet and spectrum correlation assessment for locomotive bearing fault diagnosis," *Sensors*, vol. 13, no. 11, pp. 15726–15746, Nov. 2013.

[35] H. Liu C. Xiang, and S. Fu, "Research on dynamic coupled characteristics of a tracked vehicle gearbox," *Int. J. Comput. Intell. Syst.*, vol. 4, no. 6, pp. 1204–1215, 2011.

[36] R. Peled, S. Braun, and M. Zacksenhouse, "A blind deconvolution separation of multiple sources, with application to bearing diagnostics," *Mech. Syst. Signal Process.*, vol. 19, no. 6, pp. 1181–1195, 2005.

MANG GAO was born in 1990. He received the B.S. degree in petroleum engineering from Yangtze University (Jinzhou), China, in 2012. He is currently pursuing the master's degree with the Harbin Institute of Technology at Shenzhen, Shenzhen, China.

His research interests include the fault diagnosis and prognosis, condition monitoring of wind turbines, signal processing, transfer learning, and machine learning applied in complex machinery systems.

GANG YU was born in 1969. He received the B.S. and master's degrees in mechanical engineering from the Dalian University of Technology, Dalian, China, in 1992 and 1995, respectively, and the Ph.D. degree in industrial and manufacturing engineering from the University of Wisconsin–Milwaukee, USA, in 2002.

Since 2005, he has been with the Harbin Institute of Technology at Shenzhen, where he is currently an Associate Professor with the School of Mechanical Engineering and Automation. His current research interests include signal processing, fault prognosis and diagnosis, condition monitoring, intelligent maintenance, and service robots.

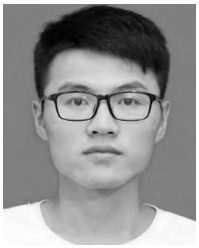

TAO WANG was born in 1994. He received the B.S. degree in mechanical engineering from the Harbin Institute of Technology at Weihai, China, in 2016. He is currently pursuing the master's degree with the Harbin Institute of Technology at Shenzhen, Shenzhen, China.

His research interests include the ultrasonic bearing and the fault diagnosis of dynamic systems.